

2D Copper(II) Complex Built from *N*-Methyl-1,3-diamino-2-propanolate and Azide Ligands: Structure, Magnetic, and DFT StudiesM. Salah El Fallah,^{*,†} Ramon Vicente,[†] Javier Tercero,[†] Christian Elpelt,[‡] Eva Rentschler,[‡] Xavier Solans,^{§,||} and Mercè Font-Bardia[§]

Departament de Química Inorgànica, Universitat de Barcelona, Martí i Franquès, 1-11, 08028-Barcelona, Spain, Institut für Anorganische Chemie and Analytische Chemie, Johannes Gutenberg Universität of Mainz, Duesbergweg 10-14, 55099-Mainz, Germany, and Departament de Cristal·lografia i Mineralogia, Universitat de Barcelona, Martí i Franquès s/n, 08028-Barcelona, Spain

Received March 17, 2008

The synthesis, structural characterization, and magnetic behavior of a new 2D copper(II) compound with formula $\{[\text{Cu}_2(\mu\text{-O}_2\text{CMe})(\mu\text{-MedapO})(\mu_{1,1}\text{-N}_3)_2]_n(\text{CH}_3\text{OH})_n\}$ **1**, in which MedapOH is *N*-methyl-1,3-diamino-2-propanol is reported herein. **1** crystallizes in the triclinic system, space group $P\bar{1}$, with unit cell parameters $a = 6.688(5)$ Å, $b = 10.591(6)$ Å, $c = 12.100(7)$ Å, $\alpha = 113.01(3)^\circ$, $\beta = 105.08(4)^\circ$, $\gamma = 93.93(3)^\circ$, $Z = 2$. The structure of **1** consists of neutral alternate 1D chains formed by the sequence of $[\text{Cu}(1)-(\mu_{1,1}\text{-N}_3)_2-\text{Cu}(1)-(\text{MedapO}/\text{acetate})-\text{Cu}(2)-(\mu_{1,1}\text{-N}_3)_2-\text{Cu}(2)]$. Each dinuclear $[\text{Cu}(1)-\text{Cu}(2)]$ unit interacts with similar dinuclear units of neighbor chains in basis to large Cu–N(azido) distances to give a 2D arrangement. The magnetic behavior of **1** has been checked giving a net ferromagnetic coupling. The fit of the χ_M versus T data as dinuclear compound affords a J value of 53.0 cm^{-1} as a consequence of the orbital countercomplementarity phenomenon. The exchange pathways have been justified by density functional calculations.

Introduction

In dinuclear copper(II) complexes bridged by a pair of hydroxide or alkoxide oxygen atoms the value and sign of the J coupling is mainly dependent on the Cu–O–Cu bridge angle. In a yet classical paper, Hatfield and Hodgson¹ have published a linear correlation for homobridged $[\text{Cu}(\mu\text{-OH})_2\text{Cu}]^{2+}$ dinuclear compounds between the experimental exchange coupling constant and the Cu–O–Cu bond angle (θ). Dinuclear compounds with θ larger than 97.6° are antiferromagnetically coupled, whereas the coupling is ferromagnetic if θ is lower than 97.6° . For θ larger than 97.6° , the $|J|$ value increases with increasing θ . In heterobridged dinuclear copper(II) systems in which one hydroxo or alkoxo bridge has been substituted by one syn–syn carboxylate

bridging ligand, a lowering of the $|J|$ value can be observed with reference to the homobridged one with the same Cu–O–Cu angle.² This effect has been called the orbital counter-complementarity phenomenon.³ Even in the heterobridged dinuclear copper(II) systems, positive J values have been observed when the Cu–O–Cu angles are in the range of $110\text{--}107^\circ$.^{4–7}

In a recent work,⁸ we have studied the countercomplementarity phenomenon in a series of four structurally related dinuclear $[\text{Cu}_2\text{L}(\mu_2\text{-acetato})]^{2+}$ units ($\text{L} = \mu\text{-bdmapO}$ or $\mu\text{-bdapO}$). BdmapOH = 1,3-bis(dimethylamino)-2-propanolate and bdapOH = 1,3-bis(amino)-2-propanolate are polytopic anionic ligands containing anchoring N-donor atoms

* To whom correspondence should be addressed. E-mail: salah.elfallah@qi.ub.es; Fax: +34 93 490 7725.

[†] Departament de Química Inorgànica, Universitat de Barcelona.

[‡] Institut für Anorganische Chemie and Analytische Chemie, Johannes Gutenberg-Universität of Mainz.

[§] Departament de Cristal·lografia i Mineralogia, Universitat de Barcelona.

^{||} Deceased in September, 2007.

(1) Crawford, V. H. R.; Richardson, H. W.; Wasson, J. R.; Hodgson, D. J.; Hatfield, W. E. *Inorg. Chem.* **1976**, *15*, 2107.

(2) Nishida, Y.; Kida, S. *J. Chem. Soc., Dalton Trans.* **1986**, 2633.

(3) Kahn, O. *Molecular Magnetism*, VCH Publishers: New York, 1993.

(4) Gutierrez, L.; Alzuet, G.; Real, J. A.; Cano, J.; Borrás, J.; Castiñeiras, A. *Inorg. Chem.* **2000**, *39*, 3608.

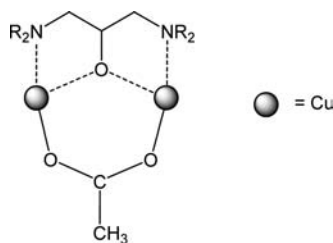
(5) Gutierrez, L.; Alzuet, G.; Real, J. A.; Cano, J.; Borrás, J.; Castiñeiras, A. *Eur. J. Inorg. Chem.* **2002**, 2094.

(6) Thompson, L. K.; Tandon, S. S.; Lloert, F.; Cano, J.; Julve, M. *Inorg. Chem.* **1997**, *36*, 3301.

(7) Tudor, V.; Kravtsov, V. Ch.; Julve, M.; Lloret, F.; Simonov, Y. A.; Averkiev, B. B.; Andruh, M. *Inorg. Chem. Acta* **2005**, *358*, 2066.

(8) El Fallah, M. S.; Badyine, F.; Vicente, R.; Escuer, A.; Solans, X.; Font-Bardia, M. *J. Chem. Soc., Dalton Trans.* **2006**, 2934.

Scheme 1



and alkoxo units able to act as a bridge between two or three cations and widely used to generate high nuclearity compounds.^{9–24} The structure of the dinuclear $[\text{Cu}_2\text{L}(\mu_2\text{-acetato})]^{2+}$ unit is shown in scheme 1.

The antiferromagnetic interaction in the reported four new dinuclear $[\text{Cu}_2\text{L}(\mu_2\text{-acetato})]^{2+}$ units ($\text{L} = \mu\text{-bdmapO}$ or $\mu\text{-bdapO}$), expressed as $|J|$ values, is in the range 109–144 cm^{-1} . These values are smaller than that expected from their large Cu-O-Cu angles in the range 130.8–133.7° for which $|J|$ values around 400 cm^{-1} have been obtained in similar polynuclear compounds with only alkoxo bridges.^{23,24} The decrease in the $|J|$ values is associated with the counter-complementarity phenomenon.⁸

Following our work directed toward the syntheses of polynuclear copper(II) compounds derived of aminoalcohols, we have used the *N*-methyl-1,3-diamino-2-propanol (MedapOH) to check the effect of the orbital countercomplementarity phenomenon in a possible set of different structural data. With this aim we have reacted copper(II) acetate with this amino alcohol and sodium azide, and we have been able to isolate one new 2D compound with formula $\{[\text{Cu}_2(\mu\text{-O}_2\text{CMe})(\mu\text{-MedapO})(\mu_{1,1}\text{-N}_3)_2]_n(\text{CH}_3\text{OH})_n\}$, **1**, in which MedapOH is *N*-methyl-1,3-diamino-2-propanol. **1** has been structurally characterized by means of single crystal X-ray diffraction. In spite of the 2D structural pattern, **1** may be considered from the magnetic point of view as the same dinuclear $[\text{Cu}_2\text{L}(\mu_2\text{-acetato})]^{2+}$ entity. The magnetic measurements for **1**, unlike the above-mentioned series of four structurally related dinuclear $[\text{Cu}_2\text{L}(\mu_2\text{-acetato})]^{2+}$ compounds, show

ferromagnetic coupling ($J = 53.0 \pm 0.5 \text{ cm}^{-1}$). This behavior has been justified by theoretical study using DFT methods.

Experimental Section

Starting Materials. *N*-Methyl-1,3-diamino-2-propanol was prepared according to the literature method.²⁵ Copper(II) acetate monohydrate and sodium azide (Aldrich) were used as such.

Caution! *Although no incidents were recorded in this study, azido salts of metal complexes with organic ligands are potentially explosive. Only a small amount of material should be prepared, and it should be handled with care.*

Spectral and Magnetic Measurements. Infrared spectra (4000–200 cm^{-1}) were recorded from KBr pellets in a PerkinElmer 1330 IR spectrophotometer. Magnetic susceptibility measurements under magnetic fields of approximately 0.05 and 0.1 T, in the range 2–30 and 35–300 K, respectively, were performed with a Quantum Design MPMS-XL SQUID magnetometer at the Magnetochemistry Service of the University of Barcelona. All measurements were performed on polycrystalline samples. Diamagnetic corrections were estimated from Pascal Tables.

Synthesis of $\{[\text{Cu}_2(\mu\text{-O}_2\text{CMe})(\mu\text{-MedapO})(\mu_{1,1}\text{-N}_3)_2]_n(\text{CH}_3\text{OH})_n\}$ **1.** To a turquoise solution of 0.401 g (2 mmol) of $\text{Cu}(\text{CH}_3\text{COO})_2 \cdot \text{H}_2\text{O}$ in 20 mL of methanol, 0.105 g (1 mmol) of *N*-methyl-1,3-diamino-2-propanol in 20 mL of methanol was added, and a dark-blue solution was formed. After 5 min of stirring, 0.132 g (2 mmol) of sodium azide were added and a dark green solution was formed. After stirring for 30 min and subsequent air filtration, slow evaporation of the green solution yielded green crystals suitable for X-ray determination after 1 day. FTIR (KBr): $\lambda^{-1} = 2054$ [ν_{as} (NNN)], 1559 [ν_{as} (COO)], 1428 [ν_{s} (COO)] cm^{-1} . The elemental analyses (carbon, nitrogen, and hydrogen) was consistent with the product formulation: (Found: C, 21.0; H, 4.5; N, 26.9%. Calcd For $\text{C}_7\text{H}_{18}\text{Cu}_2\text{N}_8\text{O}_4$: C, 20.7; H, 4.5; N, 27.6%.

X-ray Crystallography. A good quality crystal of **1** was selected and mounted on a MAR345 diffractometer with an image plate detector. The crystallographic data, conditions retained for the intensity data collection, and some features of the structure refinements are listed in Table 1. The accurate unit-cell parameters were determined from automatic centring of 131 ($3 < \theta < 31^\circ$) and refined by the least-squares method. Intensities were collected with graphite monochromated $\text{Mo K}\alpha$ radiation. Reflections (8053) were measured in the range $3.19 \leq \theta \leq 29.99$, of which 3902 reflections were nonequivalent by symmetry, R_{int} (on I) = 0.053 (1). The observed reflections applying the condition $I > 2\sigma(I)$ were 2907. Lorentz polarization and absorption corrections were made. The structure was solved by direct methods, using the *SHELXS* computer program²⁶ and refined by full-matrix least-squares method, using the *SHELX97* computer program²⁷ using 8053 reflections (very negative intensities were not assumed). The functions minimized were $\sum w[|F_o|^2 - |F_c|^2]^2$, where $w = [\sigma^2(I) + (0.0556P)^2]^{-1}$ and $P = (|F_o|^2 + 2|F_c|^2)/3$. f , f' , and f'' were taken from the International Tables of X-ray Crystallography.²⁸ Four hydrogen atoms were located from difference synthesis and 14 other hydrogen atoms were computed and refined, using a riding model, with an isotropic temperature factor equal to 1.2 times the equivalent

- (9) (a) Kivekas, R. *Finn. Chem. Lett.* **1974**, 39. (b) Kivekas, R. *Finn. Chem. Lett.* **1977**, 252.
 (10) Kivekas, R. *Cryst. Struct. Commun.* **1977**, 6, 483.
 (11) Kivekas, R. *Finn. Chem. Lett.* **1978**, 71.
 (12) Pajunen, A.; Kivekas, R. *Cryst. Struct. Commun.* **1979**, 8, 385.
 (13) Wang, S.; Smith, K. D. L.; Pang, Z.; Wagner, M. J. *Chem. Commun.* **1992**, 1594.
 (14) Wang, S.; Trepanier, S. J.; Zheng, J. C.; Pang, Z.; Wagner, M. J. *Inorg. Chem.* **1992**, 31, 2118.
 (15) Wang, S.; Pang, Z.; Smith, K. D. L. *Inorg. Chem.* **1993**, 32, 4992.
 (16) Wang, S.; Trepanier, S. J.; Wagner, M. J. *Inorg. Chem.* **1993**, 32, 833.
 (17) Wang, S.; Pang, Z.; Zheng, J. C.; Wagner, M. J. *Inorg. Chem.* **1993**, 32, 5975.
 (18) Pang, Z.; Smith, K. D. L.; Wagner, M. J. *J. Chem. Soc., Dalton Trans.* **1994**, 955.
 (19) Breeze, S. R.; Wang, S.; Thompson, L. K. *Inorg. Chim. Acta* **1996**, 250, 163.
 (20) Ribas, J.; Monfort, M.; Costa, R.; Solans, X. *Inorg. Chem.* **1993**, 32, 695.
 (21) El Fallah, M. S.; Rentschler, E.; Caneschi, A.; Sessoli, R.; Gatteschi, D. *Inorg. Chem.* **1996**, 35, 3723.
 (22) Fleeting, K. A.; O'Brien, P.; Jones, A. C.; Otway, D. J.; White, A. J. P.; Williams, D. J. *J. Chem. Soc., Dalton Trans.* **1999**, 2853.
 (23) El Fallah, M. S.; Escuer, A.; Vicente, R.; Badyine, F.; Solans, X.; Font-Bardía, M. *Inorg. Chem.* **2004**, 43, 7218.
 (24) Escuer, A.; El Fallah, M. S.; Vicente, R.; Sanz, N.; Font-Bardía, M.; Solans, X.; Mautner, F. A. *J. Chem. Soc., Dalton Trans.* **2004**, 1867.

- (25) Satcher, J. H.; Droegge, M. W.; Weakley, T. J. R.; Taylor, R. T. *Inorg. Chem.* **1995**, 34, 3317.
 (26) Sheldrick, G. M. *SHELXS, A Program Automatic Solution of Crystal Structures*; Universität Göttingen: Göttingen, Germany, 1997.
 (27) Sheldrick, G. M. *SHELXL-97, A Program for Crystal Structure Refinement*; Universität Göttingen, Göttingen, Germany, 1997.
 (28) *International Tables of X-ray Crystallography*; Kynoch Press, 1974; Vol. IV, pp 99–100 and 149.

Table 1. Crystal Data and Structure Refinement for $\{[\text{Cu}_2(\mu\text{-O}_2\text{CMe})(\mu\text{-MedapO})(\mu_{1,1}\text{-N}_3)_2]_n(\text{CH}_3\text{OH})_n\} \mathbf{1}$

compound	1
empirical formula	C ₇ H ₁₈ Cu ₂ N ₈ O ₄
fw	405.37
T (K)	293(2)
wavelength (Å)	0.71073
cryst syst/space group	triclinic/ <i>P</i> $\bar{1}$
unit cell dimensions, a (Å)	6.688(5)
b (Å)	10.591(6)
c (Å)	12.100(7)
α (°)	113.01(3)
β (°)	105.08(4)
γ (°)	93.93(5)
V (Å ³)	747.6(8)
Z, D _{calcd} (mg/m ³)	2, 1.801
absorption coefficient (mm ⁻¹)	2.873
F(000)	412
cryst size (mm ³)	0.2 × 0.1 × 0.1
theta range for data collection (°)	3.19 to 29.99
index ranges	-9 ≤ h ≤ 9, -15 ≤ k ≤ 15, -18 ≤ l ≤ 18
reflins collected	8053
independent reflins	3902 [R(int) = 0.0531]
refinement method	Full-matrix least-squares on F ²
data/restraints/params	3902/13/204
GOF on F ²	1.073
final R indices [I > 2σ(I)]	R1 = 0.0449, wR2 = 0.1070
R indices (all data)	R1 = 0.0651, wR2 = 0.1139
largest diff. peak and hole (e.Å ⁻³)	0.567 and -0.375

temperature factor of the atoms, which are linked. The final *R* (on *F*) factor was 0.045; *wR* (on |*F*_o|²) was 0.107. The molecular plots were obtained using the *Ortep32* program.²⁹

Results and Discussion

Description of the Structure of $\{[\text{Cu}_2(\mu\text{-O}_2\text{CMe})(\mu\text{-MedapO})(\mu_{1,1}\text{-N}_3)_2]_n(\text{CH}_3\text{OH})_n\} \mathbf{1}$. The *ORTEP* drawing of the structure of **1** is illustrated in part (A) of Figure 1. Selected bonds lengths and angles are listed in Table 1. The structure of **1** consists of neutral alternate 1D chains (part (B) of Figure 1), where the sequence of metal centers within the chain is [Cu(1)-(μ_{1,1}-N₃)₂-Cu(1)-(MedapO/acetate)-Cu(2)-(μ_{1,1}-N₃)₂-Cu(2)]. However, each dinuclear [Cu(1)-Cu(2)] unit interacts with similar dinuclear units of neighbor chains in basis to large Cu-N(azido) distances to give a 2D arrangement as it is shown in part (C) of Figure 1. The Cu(1)-N(8)#3 and Cu(2)-N(8)#3 distances are, respectively, 2.858(5) and 2.929(5) Å. The coordination mode of the azido ligands can be structurally described as μ-1,1,3,3. In the compound, the nearest-neighbor Cu...Cu distances are 3.192(2), 3.337(3), 3.378(3), 5.284(4), and 6.664(5) Å, corresponding to the five sets of one MedapO/acetate, two di-μ_{1,1}-azide, and two mono-μ_{1,1,3,3}-azide bridges, respectively. In each [Cu(1)-(MedapO/acetate)-Cu(2)]²⁺ dinuclear unit, the copper(II) atoms are bridged by one oxygen atom from the μ-MedapO ligand and one μ-*syn-syn*-acetate ligand. The coordination around the Cu(1) and Cu(2) centers is distorted octahedral. The equatorial plane around Cu(1) is formed by O(1) and N(1) (MedapO ligand), O(2) (acetato), and N(6) (azide bridge). The axial positions are occupied by the N(6)#2 and N(8)#3 atoms of two bridging azide ligands. Around Cu(2), the equatorial plane is formed by O(1) and N(2) (MedapO ligand), O(3) (acetato), and N(3) (bridging azide). The two axial positions are occupied by the N(3)#1 and N(8)#3 atoms of two bridging azide ligands. On the other hand, it is interesting to notice in this structure the low value found for the

Table 2. Relevant Bond Lengths [Angstroms] and Angles [Degrees] for $\{[\text{Cu}_2(\mu\text{-O}_2\text{CMe})(\mu\text{-MedapO})(\mu_{1,1}\text{-N}_3)_2]_n(\text{CH}_3\text{OH})_n\} \mathbf{1}^a$

Cu(1)-O(1)	1.937(3)	Cu(2)-O(1)	1.950(3)
Cu(1)-O(2)	1.963(3)	Cu(2)-O(3)	1.962(3)
Cu(1)-N(6)	2.007(3)	Cu(2)-N(3)	1.979(3)
Cu(1)-N(1)	2.049(3)	Cu(2)-N(2)	2.046(3)
Cu(1)-N(6)#2	2.583(4)	Cu(2)-N(3)#1	2.596(4)
Cu(1)-N(8)#3	2.858(5)	Cu(2)-N(8)#3	2.929(5)
Cu(1)...Cu(2)	3.192(2)	Cu(2)...Cu(2)#1	3.378(3)
Cu(1)...Cu(1)#2	3.337(3)	Cu(2)...Cu(1)#3	6.664(5)
Cu(1)...Cu(1)#3	5.284(4)		
O(1)-Cu(1)-O(2)	94.9(1)	O(1)-Cu(2)-O(3)	91.9(1)
O(1)-Cu(1)-N(1)	86.3(1)	O(1)-Cu(2)-N(2)	84.7(1)
O(1)-Cu(1)-N(6)	172.3(1)	O(1)-Cu(2)-N(3)	177.3(1)
O(1)-Cu(1)-N(6)#2	99.9(1)	O(1)-Cu(2)-N(3)#1	96.6(1)
O(1)-Cu(1)-N(8)#3	85.7(1)	O(1)-Cu(2)-N(8)#3	83.5(1)
O(2)-Cu(1)-N(1)	171.5(1)	O(3)-Cu(2)-N(2)	176.3(1)
O(2)-Cu(1)-N(6)	87.4(1)	O(3)-Cu(2)-N(3)	89.4(1)
O(2)-Cu(1)-N(6)#2	84.5(1)	O(3)-Cu(2)-N(3)#1	91.6(1)
O(2)-Cu(1)-N(8)#3	88.3(1)	O(3)-Cu(2)-N(8)#3	96.5(1)
N(1)-Cu(1)-N(6)	92.6(1)	N(2)-Cu(2)-N(3)	94.1(1)
N(1)-Cu(1)-N(6)#2	87.0(1)	N(2)-Cu(2)-N(3)#1	87.5(1)
N(1)-Cu(1)-N(8)#3	100.2(1)	N(2)-Cu(2)-N(8)#3	84.4(1)
N(6)-Cu(1)-N(6)#2	87.6(1)	N(3)-Cu(2)-N(3)#1	85.79(13)
N(6)-Cu(1)-N(8)#3	86.9(1)	N(3)-Cu(2)-N(8)#3	93.94(14)
N(6)#2-Cu(1)-N(8)#3	171.2(1)	N(3)#1-Cu(2)-N(8)#3	171.9(1)
Cu(1)-N(6)-N(7)	119.4(3)	Cu(2)-N(3)-N(4)	122.0(3)
Cu(1)-N(6)-Cu(1)#2	92.4(1)	Cu(2)-N(3)-Cu(2)#1	94.2(1)
Cu(1)#2-N(6)-N(7)	113.9(3)	Cu(2)#1-N(3)-N(4)	112.1(3)
Cu(1)#3-N(8)-N(7)	111.3(3)	Cu(2)#3-N(8)-N(7)	144.6(4)
Cu(1)#3-N(8)-Cu(2)#3	66.9(1)	Cu(1)-O(1)-Cu(2)	110.4(1)
N(6)-N(7)-N(8)	178.4(4)	N(3)-N(4)-N(5)	174.8(4)

^a Symmetry transformations used to generate equivalent atoms: #1: 1 - x, -y, -z; #2: 1 - x, 1 - y, 1 - z; #3: 2 - x, 1 - y, 1 - z.

Cu(1)-O(1)-Cu(2) angle, being 110.4(1)°, if it is compared to a similar fragment in the structures reported in the literature.^{6,19,21,22} The dihedral angle (λ) between the adjacent basal planes such as O(1)-O(3)-N(3)-N(2) and O(1)-O(2)-N(6)-N(1) is equal to 62.9(1)°.

Magnetic Study. The magnetic behavior of **1** is shown in Figure 2, as a $\chi_{\text{M}}T$ versus *T* plot for dinuclear unit. At room temperature, the $\chi_{\text{M}}T$ value is 0.933 cm³·K mol⁻¹, which is close to the expected value for two uncoupled copper(II) ions with *g* = 2.23. $\chi_{\text{M}}T$ increases slightly with lowering of temperature and reaches a maximum of 1.112 cm³·K mol⁻¹ ca. 20 K. Below this temperature, $\chi_{\text{M}}T$ decreases to a value of 0.702 cm³·K mol⁻¹ at 2 K. The shape of this curve indicates dominant ferromagnetic coupling until 20 K.

As it is shown in part (C) of Figure 1, the structure of **1** consists of copper ions linked between them by MedapO/acetate and azide ligands to give a bidimensional compound. To interpret the magnetic behavior of **1**, we assume a negligible contribution from the weak axial interactions through the azide bridges due to the long Cu(1)-N(8)#3 and Cu(2)-N(8)#3 distances (2.858(5) and 2.929(5) Å, respectively). The system may be treated in a simplified form as an alternate chain of Cu(II) atoms (part (B) of Figure 1). Because of the very slight variations between two successive (μ_{1,1}-N₃)₂ bridges in the same chain, they are two different coupling constants to consider along the chain, *J*₁ and *J*₂, which correspond to the MedapO/acetate and di-μ_{1,1}-azide bridges respectively. As an approach to the *J* coupling constants, a fit based on the interaction Scheme 2 was performed by means of the computer program *CLUMAG*³⁰ using the Hamiltonian *H*, assuming the already know fact that a 12-membered ring of S=1/2 describes satisfactorily the magnetic behavior of the chain:³¹

$$H = -J_1(S_1S_2 + S_3S_4 + S_5S_6 + S_7S_8 + S_9S_{10} + S_{11}S_{12}) - J_2(S_2S_3 + S_4S_5 + S_6S_7 + S_8S_9 + S_{10}S_{11} + S_{12}S_1)$$

The best fit parameters found were $J_1 = +53.0 \pm 0.5 \text{ cm}^{-1}$, $J_2 = -1.9 \pm 0.2 \text{ cm}^{-1}$, and $g = 2.17$. Taking into account the relatively low J_2 value, we can consider that the magnetic coupling is mainly dominated by the strongest interaction J_1 , propagated through the MedapO/acetate bridge. The low J_2 value can be associated to the di- $\mu_{1,1}$ -azide bridge due to the long Cu(1)–N(6)#2 and Cu(2)–N(3)#1

distances (2.583(4) and 2.596(4) Å, respectively). This consideration reduces the system to magnetically isolated dinuclear units in the compound.

To prove this possibility, the experimental magnetic data were fitted again by using the Bleaney–Bowers expression for an isotropically coupled pair of $S = 1/2$ ions [(eq 1)] in conjunction with an additional mean-field correction term, χ_{MF} , [eq (2)] where N is Avogadro's number, μ_B is the Bohr magneton, k_B is the Boltzmann constant, and z is the number

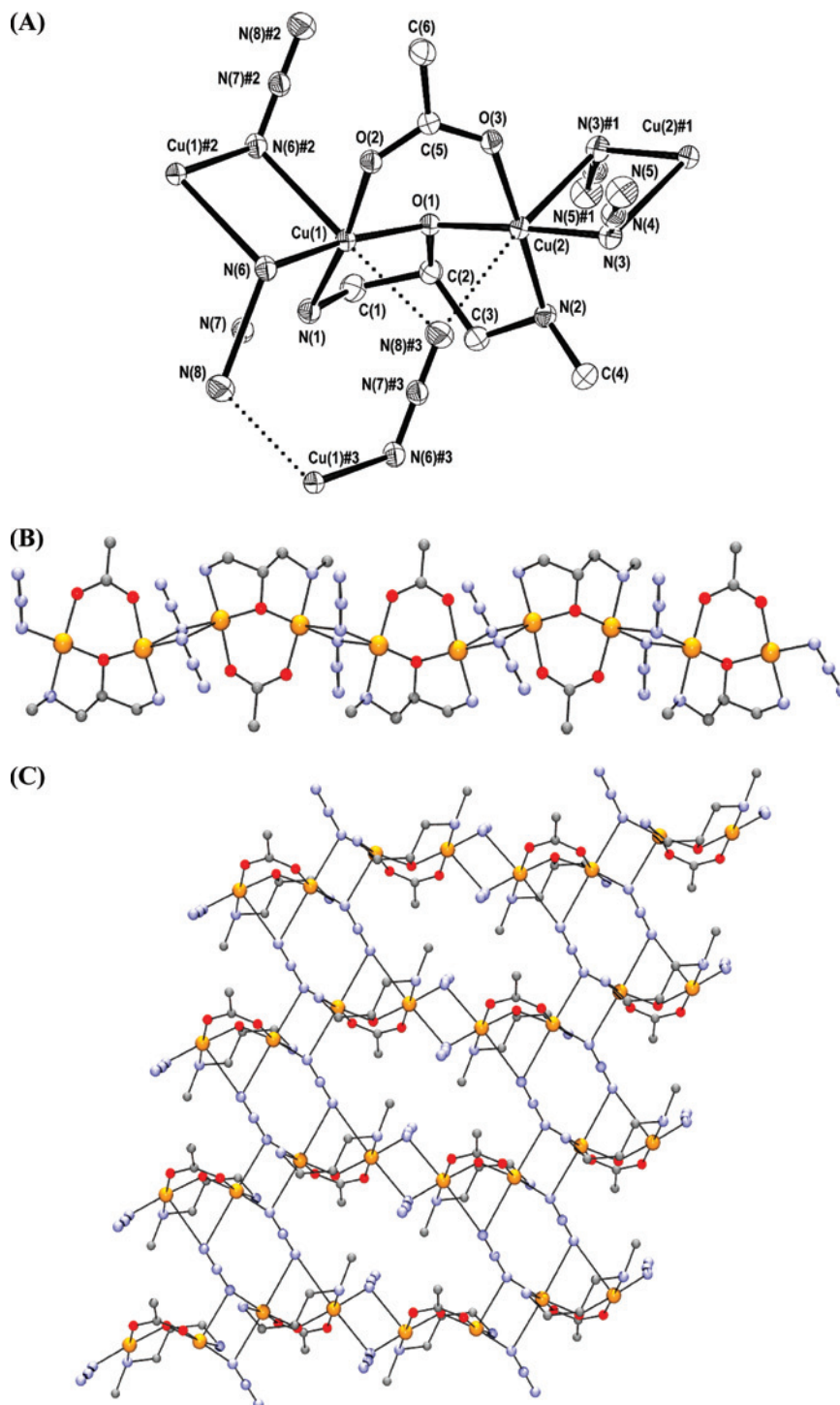


Figure 1. (a) ORTEP drawing of the structure of **1** showing atom labeling scheme. Ellipsoids at the 50% probability level. (Symmetry transformations used to generate equivalent atoms: #1: $1 - x, -y, -z$; #2: $1 - x, 1 - y, 1 - z$; #3: $2 - x, 1 - y, 1 - z$.) (b) Drawing of the alternate chain [$-\mu_{1,1}$ -(N₃)₂-Cu(1)-(MedapO/acetate)-Cu(2)- $\mu_{1,1}$ -(N₃)₂-] in **1**. (c) 2D arrangement in **1**.

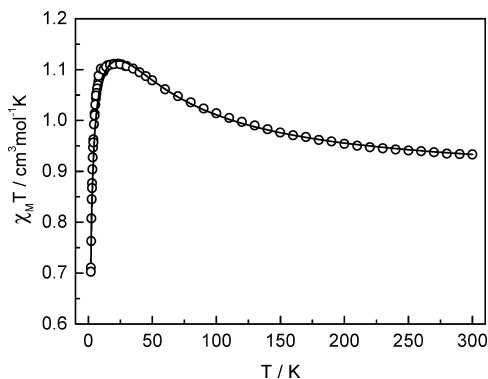
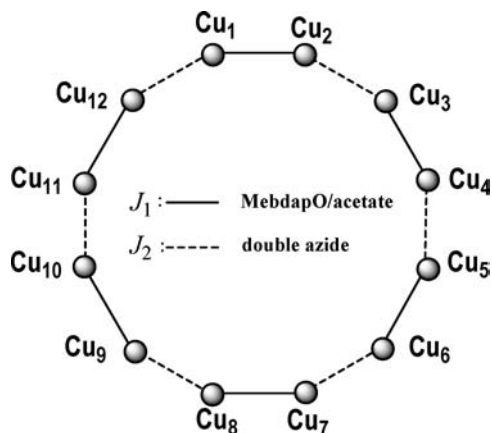


Figure 2. Plot of observed $\chi_M T$ vs T of **1**. Solid line represents the best theoretical fit using the CLUMAG program (text).

Scheme 2. Schematic Diagram Representing the Exchange Interactions within **1**



of nearest neighbors. The best fit parameters were $J_1 = +50.8 \pm 0.4 \text{ cm}^{-1}$, $zJ' = -0.95 \pm 0.03 \text{ cm}^{-1}$, and $g = 2.17$ with $R = 3.4 \times 10^{-5}$ ($R = \sum_i (\chi T_{\text{icalc}} - \chi T_{\text{ieptl}})^2 / (\chi T_{\text{ieptl}})^2$).

$$\chi_M = \frac{Ng^2\mu_B^2}{k_B T} \frac{2 \exp(J/k_B)}{1 + 3 \exp(J/k_B)} \quad (1)$$

$$\chi_{MF} = \frac{\chi_M}{1 - \chi_M (zJ'/Ng^2\mu_B^2)} \quad (2)$$

As we observe, the J value found is very similar to J_1 , which confirms that **1** can be considered, from the magnetic point of view, as a dinuclear compound up to 20 K. The $\chi_M T$ decreasing observed at low temperature may be due to the interdimer antiferromagnetic exchange and/or the presence of the ZFS of the ground state.

Theoretical Study Using DFT Methods. Contrary to the series of antiferromagnetic complexes reported by the authors,⁸ **1** shows ferromagnetic behavior even having the similar structural unit $[\text{Cu}_2\text{L}(\mu_2\text{-acetato})]^{2+}$. With the aim to justify this difference we have performed theoretical calculations based on density functional theory (DFT) using the Cartesian coordinates of a tetranuclear model based on the crystal structure data of **1**. The tetranuclear model corresponds to the elemental unit necessary to determine the two possible interactions J_1 and J_2 as has been commented previously (Figure 3). DFT calculations give the following results: $J_1 = +58.2 \pm 0.1 \text{ cm}^{-1}$ and $J_2 = -1.0 \pm 0.2 \text{ cm}^{-1}$, indicating similar values

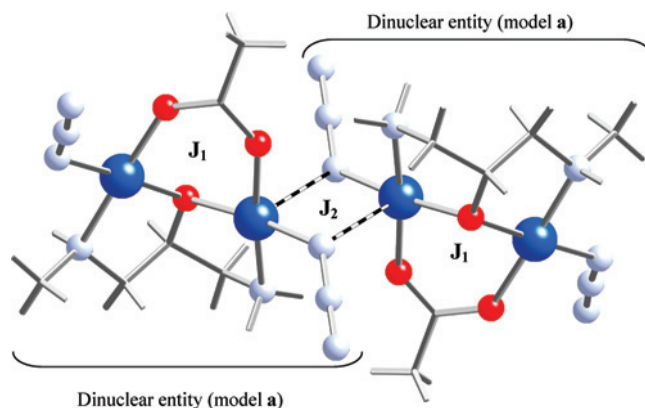


Figure 3. Structural representation of the tetranuclear model showing the exchange coupling constants J_1 and J_2 . Multiband cylinder bonds indicate the longer distance Cu–N (2.58 Å).

to those found above ($J_1 = +53.0 \text{ cm}^{-1}$ and $J_2 = -1.9 \text{ cm}^{-1}$). All of the details concerning the DFT calculation are reported in the computational methodology paragraph.

To understand the exchange mechanism through each bridging ligand, we have calculated the different coupling constant values J_1 and J_2 separately, considering the following dinuclear models: (a) J_1 in $[\text{Cu}(\text{MedapO}/\text{acetate})\text{-Cu}]$; in this case J_1 should be the result of the two contributions (alkoxo bridge of the aminoalcohol ligand and the acetate ligand). (b) J_1 in $[\text{Cu}(\text{H}_2\text{O})\text{-(MedapO)-Cu}(\text{H}_2\text{O})]$, where we have substituted the acetate ligand by two water molecules, in this situation there is only one exchange pathway; (alkoxo bridge). (c) J_2 in $[\text{Cu}(\mu_{1,1}\text{-N}_3)_2\text{-Cu}]$, where the J_2 coupling constant should be the result of the contribution of a double asymmetric end-on azide ligand.

The calculated exchange coupling constants by DFT method for the model (a) and model (b) were $J_1 = +52 \text{ cm}^{-1}$ and -26 cm^{-1} , respectively. The variation of J_1 observed between the two models can be interpreted by considering the Hay–Thibeault–Hoffmann expression (eq 3).³² If the coupling constant is given by,

$$J = 2K_{\text{ab}} - \frac{(\epsilon_1 - \epsilon_2)^2}{J_{\text{aa}} - J_{\text{ab}}} = J_{\text{F}} + J_{\text{AF}} \quad (3)$$

the J_{AF} term will be probably smaller in the model (a), considering the relative small Cu–O–Cu angle (110.4°) compared with the same Cu–O–Cu found in previous similar antiferromagnetic complexes (ranging from 130.8 to 138.9°).^{8,23} In this situation, we should expect the first term, $2K_{\text{ab}}$, to dominate, giving an overall positive value for the coupling constant, $+52 \text{ cm}^{-1}$ ($+58 \text{ cm}^{-1}$ calculated for the tetranuclear model). However, in model (b), the second term

(29) Farrugia, L. J. *J. Appl. Crystallogr.* **1997**, *30*, 565.

(30) The series of calculations were made using the computer program CLUMAG, which uses the irreducible tensor operator formalism (ITO) Gatteschi, D.; Pardi, L. *Gazz. Chim. Ital.* **1993**, *123*, 231.

(31) (a) Bary, J. W.; Interrante, L. W.; Jacobs, I. S.; Bonner, J. C. *Extended Linear Chain Compounds*; Miller, S., Ed.; Plenum: New York, 1983; Vol. 3. (b) Borrás-Almenar, J. J.; Coronado, E.; Curely, J.; Georges, R.; Gianduzzo, J. C. *Inorg. Chem.* **1994**, *33*, 5171. (c) Escuer, A.; Vicente, R.; El Fallah, M. S.; Kumar, S. B.; Mautner, F. A.; Gatteschi, D. *J. Chem. Soc., Dalton Trans.* **1998**, 3905.

(32) Hay, P. J.; Thibeault, J. C.; Hoffmann, R. *J. Am. Chem. Soc.* **1975**, *97*, 4884.

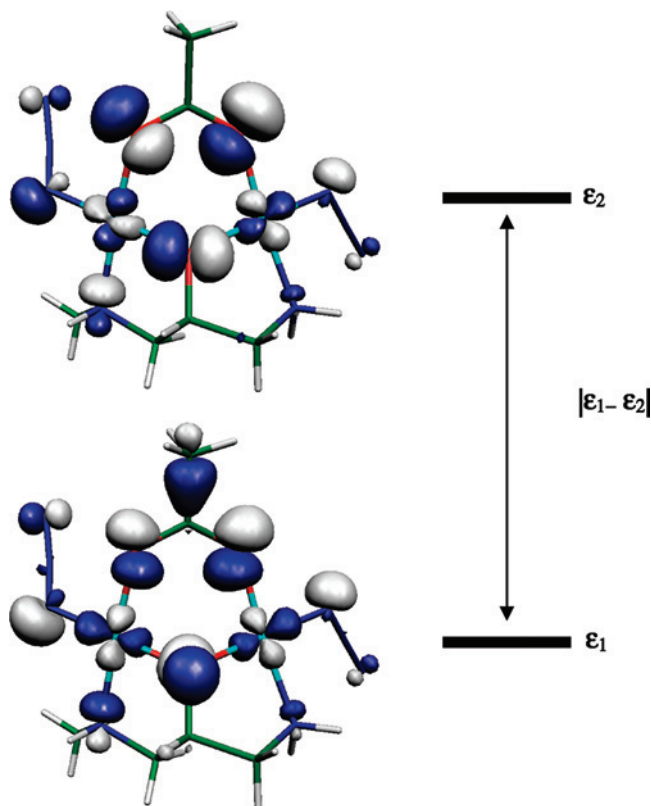


Figure 4. Representation of the two molecular orbitals bearing the unpaired electrons (SOMOs) for the model (a). The orbital with higher energy is represented above.

of the expression (eq 3) dominates, leading to an antiferromagnetic interaction (-26 cm^{-1}). These results can be illustrated by analyzing the energy gap of singly occupied molecular orbitals (SOMOs) in the models (a) and (b) (Figure 4). The presence of all of the bridging ligands reduces the energy gap, $\|\epsilon_1 - \epsilon_2\|$, from 0.007 au in model (a) to 0.005 au in model (b). This fact is due to the counter-complementation^{4,33,34} of the bridging ligands in the exchange coupling. Thus, we can conclude that the ferromagnetic interaction, J_1 , is due to the sum of two circumstances: (i) the small Cu–O–Cu angle of 110.4° in the alkoxo bridge and (ii) the counter-complementary effect of the acetate bridge.

In the model (c), the magnetic coupling through the double asymmetric end-on azide ligand is usually small, and this may be ferro or antiferromagnetic.³⁵ In our case the calculated antiferromagnetic interaction (-1.0 cm^{-1}) agree with a previous theoretical studies reported on $\mu_{1,1}\text{-N}_3$ asymmetric double bridges with one large Cu–N distance.³⁵

The analysis of the spin-density distribution in the tetranuclear model shows the predominance of a delocalization mechanism in the coordinated atoms to the copper ions as shown in the Figure 5. This is logical, considering the electronic configuration of the copper(II) cation bearing the

unpaired electron in M–L antibonding orbitals.³⁶ The spin population on the copper atoms is around $0.57 e^-$ (Figure 5), and the missing spin density, relative to one unpaired electrons, appears mainly delocalized over the bridging ligands. There is a large amount of spin population at the oxygen atom of the aminoalcohol ($0.14 e^-$), in the nitrogen atoms of the azide bridges ($0.096 e^-$), and in the oxygen atoms ($0.084 e^-$) of the acetate bridges, showing the important role (previously mentioned) of this ligand in the J_1 exchange coupling. The spin-polarization mechanism only appears to be responsible for a very small negative spin population value on some carbon atoms ($-0.003 e^-$) and of negative values in the central nitrogen atom of the azide ligands ($-0.03 e^-$). In the two cases, the negative spin population is not detected in Figure 5 due to the employed $0.02 e^-/\text{bohr}^3$ cutoff value.

Computational Methodology

DFT Calculation. To calculate the exchange coupling constants for any polynuclear complex with n different exchange constants, at least the energy of $n + 1$ different spin configurations must be calculated. When more than $n + 1$ spin distributions were calculated, a fitting procedure was necessary to obtain the coupling constants. The followed computational strategy to calculate the exchange coupling constants in dinuclear or polynuclear transition-metal complexes was described in previous works.³⁷ The exchange coupling constants are introduced by a phenomenological Heisenberg Hamiltonian $H = -\sum J S_i \cdot S_j$ (where i and j make reference to the different paramagnetic centers) to describe the interactions between the two paramagnetic transition-metal atoms. In the case of the studied tetranuclear model, the two J values have been obtained by calculating the corresponding energy of four different spin distributions (Scheme 3). The following equations have been employed to calculate the two exchange coupling constants:

$$E_{\text{LS1}} - E_{\text{HS}} = 2J_1 \quad (4)$$

$$E_{\text{LS2}} - E_{\text{HS}} = 2J_1 + J_2 \quad (5)$$

$$E_{\text{LS3}} - E_{\text{HS}} = J_2 \quad (6)$$

$$E_{\text{LS4}} - E_{\text{HS}} = J_1 \quad (7)$$

$$E_{\text{LS5}} - E_{\text{HS}} = J_1 + J_2 \quad (8)$$

The hybrid B3LYP^{38–40} functional has been used in all calculations. This functional provides excellent results for the calculation of the exchange coupling in transition-metal complexes.⁴¹ The use of the nonprojected energy of the broken symmetry solution as the energy of the low-spin state within the DFT framework provides good results. It avoids the cancelation of the nondynamic correlation effects.⁴² We have employed a triple- ξ all-electron basis set with two p-type polarization functions for copper atoms⁴³ and a double- ξ all electron for the other elements proposed by Schaefer et al.⁴⁴ All energy calculations were performed including 10^{-8} density-based convergence

(33) Escuer, A.; Vicente, R.; Mautner, F. A.; Goher, M. A. S. *Inorg. Chem.* **1997**, *36*, 1233.

(34) Fondo, M.; García-Deibe, A. M.; Corbella, M.; Ruiz, E.; Tercero, J.; Sanmartín, J.; Bermejo, M. R. *Inorg. Chem.* **2005**, *44*, 5011.

(35) Triki, S.; Gómez-García, J. C.; Ruiz, E.; Sala-Pala, J. *Inorg. Chem.* **2005**, *44*, 5501, and references therein.

(36) Cano, J.; Ruiz, E.; Alvarez, S.; Verdager, M. *Comments Inorg. Chem.* **1998**, *20*, 27.

(37) Cano, J.; Costa, R.; Alvarez, S.; Ruiz, E. *J. Chem. Theory Comput.* **2007**, *3*, 782.

(38) Becke, A. D. *J. Chem. Phys.* **1993**, *98*, 5648.

(39) Becke, A. D. *Phys. Rev. A* **1988**, *38*, 3098.

(40) Lee, C.; Yang, W.; Parr, R. G. *Phys. Rev. B* **1988**, *37*, 785.

(41) Ruiz, E. *Struct. Bonding (Berlin)* **2004**, *113*, 71.

(42) Ruiz, E.; Alvarez, S.; Cano, J.; Polo, V. *J. Chem. Phys.* **2005**, *123*, 164110.

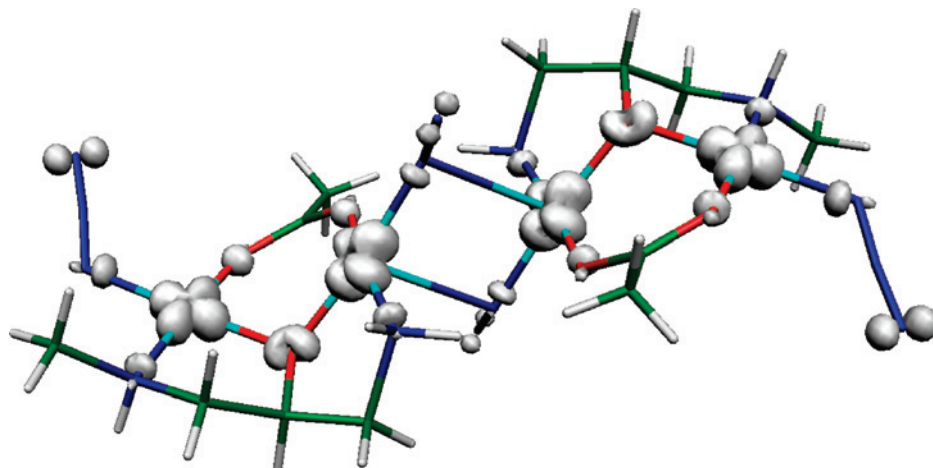
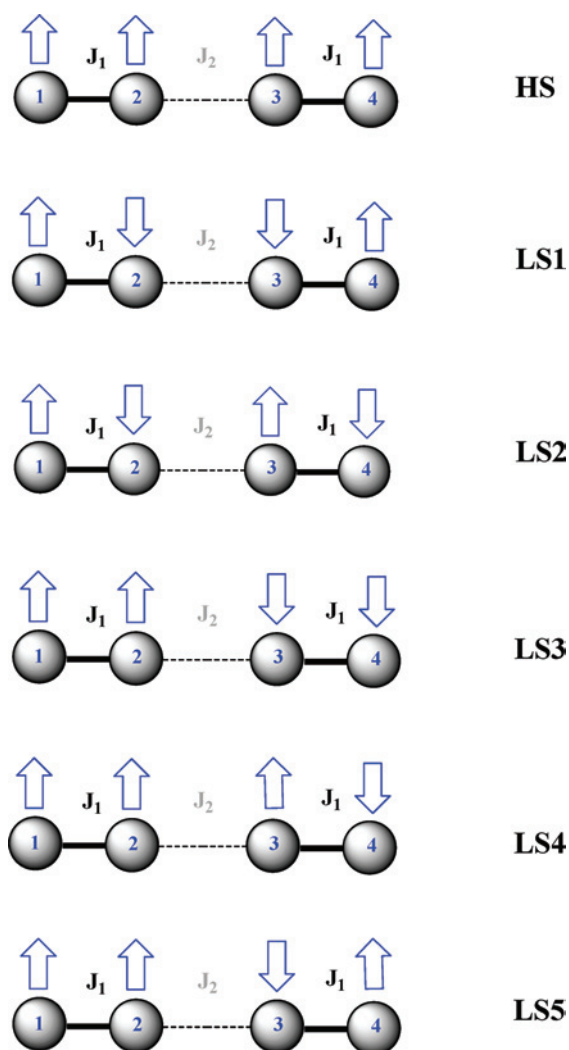


Figure 5. Spin density map for the $S = 2$ (HS) of the tetranuclear model, calculated with the B3LYP functional. Clear regions indicate positive spin populations.

Scheme 3



criterion. The calculations were performed with the *Gaussian03*⁴⁵ using guess functions generated with *Jaguar 6.0*.⁴⁶

(43) Schaefer, A.; Huber, C.; Ahlrichs, R. *J. Chem. Phys.* **1994**, *100*, 5829.
 (44) Schaefer, A.; Horn, H.; Ahlrichs, R. *J. Chem. Phys.* **1992**, *97*, 2571.

Conclusion

Here, we have presented the synthesis, crystal structure, and magnetic study of the 2D compound $\{[\text{Cu}_2(\mu\text{-O}_2\text{CMe})(\mu\text{-MedapO})(\mu_{1,1}\text{-N}_3)_2]_n(\text{CH}_3\text{OH})_n\}$ **1** obtained from copper(II) acetate, *N*-methyl-1,3-diamino-2-propanol and azido ligands. **1** behaves, from the magnetic point of view, as a dinuclear $[\text{Cu}_2\text{L}(\mu_2\text{-acetato})]^{2+}$ compound with ferromagnetic coupling ($J = 53 \text{ cm}^{-1}$). The magnetic behavior of **1** has been explained using DFT calculations, illustrating the presence of the orbital countercomplementarity phenomenon.

Acknowledgment. Financial support given by the Spanish (CTQ2006-01759, CTQ2005-08123-C02-02/BQU) and Catalan (2005SGR-00593, 2005SGR-00036) governments are acknowledged. J. Tercero is grateful to the Centre de Computació de Catalunya (CESCA) with a grant provided by Fundació Catalana per a la Recerca (FCR) and the Universitat de Barcelona. “*In Memory of Xavier Solans Huguet who left us in rough loneliness.*”

Supporting Information Available: X-ray crystallographic file including the structural data for $\{[\text{Cu}_2(\mu\text{-O}_2\text{CMe})(\mu\text{-MedapO})(\mu_{1,1}\text{-N}_3)_2]_n(\text{CH}_3\text{OH})_n\}$ **1** in CIF format. This material is available free of charge via the Internet at <http://pubs.acs.org>.

IC8004807

(45) Frisch, M. J.; Trucks, G. W.; Schlegel, H. B.; Scuseria, G. E.; Robb, M. A.; Cheeseman, J. R.; Montgomery, J. A.; Vreven, T.; Kudin, K. N.; Burant, J. C.; Millam, J. M.; Iyengar, S. S.; Tomasi, J.; Barone, V.; Mennucci, B.; Cossi, M.; Scalmani, G.; Rega, N.; Petersson, G. A.; Nakatsuji, H.; Hada, M.; Ehara, M.; Toyota, K.; Fukuda, R.; Hasegawa, J.; Ishida, H.; Nakajima, T.; Honda, Y.; Kitao, O.; Nakai, H.; Klene, M.; Li, X.; Knox, J. E.; Hratchian, H. P.; Cross, J. B.; Adamo, C.; Jaramillo, J.; Gomperts, R.; Stratmann, R. E.; Yazyev, O.; Austin, A. J.; Cammi, R.; Pomelli, C.; Ochterski, J.; Ayala, P. Y.; Morokuma, K.; Voth, G. A.; Salvador, P.; Dannenberg, J. J.; Zakrzewski, V. G.; Dapprich, S.; Daniels, A. D.; Strain, M. C.; Farkas, O.; Malick, D. K.; Rabuck, A. D.; Raghavachari, K.; Foresman, J. B.; Ortiz, J. V.; Cui, Q.; Baboul, A. G.; Clifford, S.; Cioslowski, J.; Stefanov, B. B.; Liu, G.; Liashenko, A.; Piskorz, P.; Komaromi, I.; Martin, R. L.; Fox, D. J.; Keith, T.; Al-Laham, M. A.; Peng, C. Y.; Nanayakkara, A.; Challacombe, M.; Gill, P. M. W.; Johnson, B.; Chen, W.; Wong, M. W.; Gonzalez, C. and Pople, J. A. *Gaussian 03*, Rev. B.4, Pittsburgh, PA, 2003.

(46) Schrodinger Inc. *Jaguar 6.0*, Portland, 2005.